EUROPEAN ORGANIZATION FOR NUCLEAR RESEARCH

CERN - AB DEPARTMENT

CERN-AB-2004-019 -ABP

STABILITY DIAGRAM FOR LANDAU DAMPING WITH A BEAM COLLIMATED AT AN ARBITRARY NUMBER OF SIGMAS

E. Métral and A. Verdier

Abstract

The general formula for the dispersion equation used to draw the stability diagram for Landau damping with two-dimensional betatron tune spread from octupoles is given for the nth order distribution function. It is solved in the particular case of the 15^{th} order distribution function $f(J_x, J_y) \propto [1-(J_x+J_y)/(18\sigma^2)]^{15}$, which is consistent with the nominal collimator settings in the LHC at top energy, i.e. extending up to 6σ in transverse space. The new stability diagram is compared to the ones already obtained with both the 2^{nd} order distribution function $f(J_x, J_y) \propto [1-(J_x+J_y)/(5\sigma^2)]^2$, which extends up to 3.2σ in transverse space, and the Gaussian distribution $f(J_x, J_y) \propto e^{-(J_x+J_y)/\sigma^2}$, which extends to infinity. The case of a distribution extending up to 6σ in transverse space but with more populated tails than the Gaussian is also discussed. This case may apply in reality in proton machines, where several diffusive mechanisms can take place.

Geneva, Switzerland
3 February 2004

1 INTRODUCTION

Beam stability from Landau damping in the LHC is usually evaluated for the case of the 2[nd] order (called quasi-parabolic) distribution function, which extends up to 3.2σ in transverse space [1]. This distribution function therefore underestimates the beam stability if the transverse beam profile extends up to 6σ, as it is foreseen to be the case in the LHC at top energy with the nominal collimator settings. The Gaussian distribution extends to infinity in transverse space and thus overestimates the beam stability. In this paper the beam stability is analyzed for the distribution function consistent with the collimator settings at top energy, i.e. extending up to 6σ in transverse space, and the results are compared to the ones already obtained with the above two distributions [1].

The general dispersion relation to be solved with two-dimensional betatron tune spread is given in Section 2. In Section 3, the 2[nd] order, the 15[th] order, and the Gaussian distributions are reviewed and compared. The general formulae to compute the stability diagram for the nth order and Gaussian distribution functions are given in Section 4, and solved for the 2[nd] and 15[th] orders. Finally, the case of a distribution extending up to 6σ in transverse space but with more populated tails than the Gaussian is discussed in Section 5.

2 GENERAL DISPERSION RELATION

Considering the case of a beam having the same normalized rms beam size $\sigma = \sqrt{\varepsilon}$ in both transverse planes, the Landau damping mechanism from octupoles of coherent instabilities, e.g. in the horizontal plane, is discussed from the following dispersion relation [2,3]

$$1 = -\,\Delta Q_{coh}^{x} \int_{J_x=0}^{+\infty} dJ_x \int_{J_y=0}^{+\infty} dJ_y \, \frac{J_x \dfrac{\partial f\left(J_x, J_y\right)}{\partial J_x}}{Q_c - Q_x\left(J_x, J_y\right) - m\, Q_s} \,, \qquad (1)$$

with

$$Q_x\left(J_x, J_y\right) = Q_0 + a_0\, J_x + b_0\, J_y \,. \qquad (2)$$

Here, Q_c is the coherent betatron tune to be determined, $J_{x,y}$ are the action variables in the horizontal and vertical plane respectively, with $f\,(J_x, J_y)$ the distribution function, ΔQ_{coh}^{x} is the horizontal coherent tune shift, $Q_x\,(J_x, J_y)$ is the horizontal tune in the presence of octupoles, *m* is the head-tail mode number, and Q_s is the small-amplitude synchrotron tune (the longitudinal spread is neglected).

3 NTH ORDER AND GAUSSIAN DISTRIBUTION FUNCTIONS

The nth order distribution function is given by

$$f\left(J_x,J_y\right)=a\left(1-\frac{J_x+J_y}{b}\right)^n , \tag{3}$$

where *a* and *b* are constants to be determined by normalization. The normalization of the distribution function to unity gives

$$\int_{J_x=0}^{b} dJ_x \int_{J_y=0}^{b-J_x} dJ_y\, f\left(J_x,J_y\right)=\frac{ab^2}{\left(n+1\right)\left(n+2\right)}=1 . \tag{4}$$

The average of the action variable is equal to the emittance ($<J>=\varepsilon$), which gives

$$\int_{J_x=0}^{b} J_x\, dJ_x \int_{J_y=0}^{b-J_x} dJ_y\, f\left(J_x,J_y\right)=\frac{ab^3}{\left(n+1\right)\left(n+2\right)\left(n+3\right)}=\varepsilon . \tag{5}$$

It can be deduced from Eqs. (4) and (5) that

$$b=\left(n+3\right)\varepsilon , \qquad \text{and} \qquad a=\frac{\left(n+1\right)\left(n+2\right)}{b^2} . \tag{6}$$

Following Ref. [1], the transverse beam profile, e.g. in the horizontal plane, is given by

$$\begin{aligned} g\left(x\right) &= \frac{ab}{2\pi\left(n+1\right)} \int_{-\sqrt{2b-x^2}}^{\sqrt{2b-x^2}} \left(1-\frac{x^2+p_x^2}{2b}\right)^{n+1} dp_x \\ &= \frac{2\left(n+2\right)\left[2^{n+1}\left(n+1\right)!\right]^2}{\pi\sqrt{2b}\left(2n+3\right)!}\left(1-\frac{x^2}{2b}\right)^{n+\frac{3}{2}} . \end{aligned} \tag{7}$$

As seen in Eq. (7), the profile extends up to $\sqrt{2b}$. In the case of a beam profile extending up to 6σ (due to collimator settings) the condition $\sqrt{2b}=6\sigma$ has to be satisfied, i.e. using Eq. (6), the distribution of order $n=15$ has to be considered.

The Gaussian distribution function is given by [1]

$$f\left(J_x,J_y\right)=\frac{1}{\varepsilon^2}e^{-\frac{\left(J_x+J_y\right)}{\varepsilon}} . \tag{8}$$

The corresponding transverse beam profile is given by

$$g\left(x\right)=\frac{1}{\sqrt{2\pi}\,\sigma}e^{-\frac{x^2}{2\sigma^2}} . \tag{9}$$

The transverse beam profiles for n = 2, n = 15, and for the Gaussian distribution are plotted in Fig. 1. As can be seen, the 15th order distribution function is very close to the Gaussian, which is not surprising as the closed expression for the 15th order distribution is, from Eqs. (3) and (6),

$$f\left(J_x, J_y\right) = \frac{(n+1)(n+2)}{(n+3)^2 \varepsilon^2}\left(1 - \frac{J_x + J_y}{(n+3)\varepsilon}\right)^n . \qquad (10)$$

This expression tends to Eq. (8), i.e. the Gaussian distribution function, when n tends to infinity. This can be easily found by taking the logarithm of Eq. (10) and expanding it. A zoom of the tails of the transverse beam profiles is shown on Fig. 2. It shows that the tails of both 15th order and Gaussian distributions extend further than the quasi-parabolic distribution by more than half a σ, while the tails of the 15th order distribution remain below that of the Gaussian distribution.

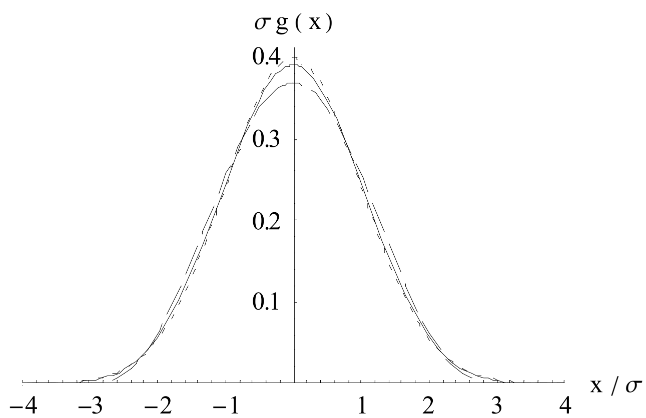

Figure 1: Transverse beam profile for the 15th order distribution (full curve), the quasi-parabolic distribution (dashed curve) and the Gaussian distribution (dotted curve).

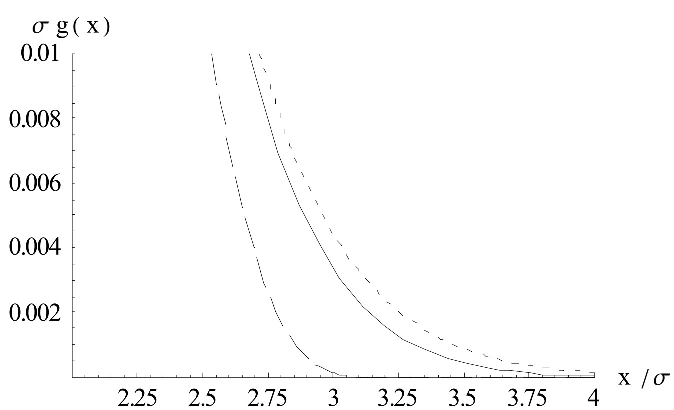

Figure 2: Zoom of the tails of the transverse beam profiles for the 15th order distribution (full curve), the quasi-parabolic distribution (dashed curve) and the Gaussian distribution (dotted curve).

4 STABILITY DIAGRAMS FOR THE NTH ORDER AND GAUSSIAN DISTRIBUTION FUNCTIONS

For the nth order distribution function, the dispersion equation of Eq. (1) can be re-written as

$$\Delta Q_{coh}^{x} = -\frac{a_0}{n\,a\,b}\, I_n^{-1}(c,q), \tag{11}$$

with

$$I_n(c,q) = \int_{J_x=0}^{1} dJ_x \int_{J_y=0}^{1-J_x} dJ_y\, \frac{J_x \left(1-J_x-J_y\right)^{n-1}}{q+J_x+c\,J_y}, \tag{12}$$

$$q = \frac{Q_c - Q_0 - m\,Q_s}{-b\,a_0}, \qquad \text{and} \qquad c = \frac{b_0}{a_0}. \tag{13}$$

For the quasi-parabolic distribution function (n = 2), which extends up to $\sqrt{10}\,\sigma \approx 3.2\,\sigma$ in transverse space, Eq. (12) gives

$$I_2(c,q) = -\left\{ \begin{array}{l} (c+q)^3\, \mathrm{Log}[1+q] - (c+q)^3\, \mathrm{Log}[c+q] + (c-1) \\ \left\{ \begin{array}{l} c\left[c + 2cq + (2c-1)\,q^2\right] \\ +(c-1)\,q^2\,(3c+q+2cq)\left(\mathrm{Log}[q] - \mathrm{Log}[1+q]\right) \end{array} \right\} \end{array} \right\} / \left[6\,(c-1)^2\, c^2\right]. \tag{14}$$

For the 15th order distribution function, which extends up to 6σ in transverse space, Eq. (12) has been solved using *Mathematica* [4] (see Eq. (A1) of Appendix 1).

In the case of the Gaussian distribution function, the dispersion equation of Eq. (1) can be re-written as

$$\Delta Q_{coh}^{x} = -\,a_0\, \varepsilon\, K^{-1}(c,p), \tag{15}$$

with

$$K(c,p) = \int_{J_x=0}^{\infty} dJ_x \int_{J_y=0}^{\infty} dJ_y\, \frac{J_x\, e^{-(J_x+J_y)}}{p+J_x+c\,J_y}, \tag{16}$$

$$p = \frac{Q_c - Q_0 - m\,Q_s}{-a_0\,\varepsilon}. \tag{17}$$

Equation (17) can be solved analytically and is given by (for $c \neq 0$) [1]

$$K(c,p) = \frac{1-c-(p+c-c\,p)\,e^{p}\,E_1(p) + c\,e^{p/c}\,E_1(p/c)}{(1-c)^2}, \tag{18}$$

where

$$E_1(z) = \int_{t=z}^{t=\infty} \frac{e^{-t}}{t} dt \tag{19}$$

is the exponential integral function.

The l.h.s of Eq. (11) or (15) contains information about the beam intensity and the impedance. The r.h.s contains information about the beam frequency spectrum. Calculation of the l.h.s is straightforward. For a given impedance, one only needs to calculate the complex mode frequency shift, in the absence of Landau damping. Without frequency spread, the condition for the beam to be stable is thus simply $\mathrm{Im}(\Delta Q_{coh}^{x}) \geq 0$ (oscillations of the form $e^{j\omega t}$ are considered).

Once its l.h.s is obtained, Eq. (11) or (15) can be used to determine the coherent betatron tune Q_c in the presence of Landau damping when the beam is at the edge of instability (i.e. Q_c real). However, the exact value of Q_c is not a very useful piece of information. The more useful question to ask is under what conditions the beam becomes unstable regardless of the exact value of Q_c under these conditions, and Eq. (11) or (15) can be used in a reversed manner to address this question. To do so, one considers the real parameter $Q_c - Q_0 - m Q_s$ (stability limit) and observes the locus traced out in the complex plane by the r.h.s of Eq. (11) or (15), as $Q_c - Q_0 - m Q_s$ is scanned form $-\infty$ to $+\infty$. This locus defines a "stability boundary diagram". The l.h.s of Eq. (11) or (15), a complex quantity, is then plotted in this plane as a single point. If this point lies on the locus, it means the solution of Q_c for Eq. (11) or (15) is real, and this $Q_c - Q_0 - m Q_s$ is such that the beam is just at the edge of instability. If it lies on the inside of the locus (the side which contains the origin), the beam is stable. If it lies on the outside of the locus, the beam is unstable. The stability diagrams for the 2nd order, 15th order and Gaussian distribution functions are plotted in Fig. 3 for the case of the LHC at top energy (7 TeV) with maximum available octupole strength ($\varepsilon = 0.5$ nm, $|a_0| = 270440$ and $c = -0.65$).

5 DISTRIBUTION WITH MORE POPULATED TAILS THAN THE GAUSSIAN

It is clear from Fig. 2 that the transverse beam profile of the Gaussian distribution is always above the one of the 15th order distribution. The latter has indeed all its derivatives up to order 16 equal to zero at 6σ. A simple way to populate the tails is to add a distribution with a smaller exponent to the nth order distribution, i.e.

$$f(J_x, J_y) = a\left(1 - \frac{J_x + J_y}{b}\right)^n + d\left(1 - \frac{J_x + J_y}{b}\right)^p, \tag{20}$$

where a, b, d, and p are constants to be determined by normalization. Here we impose that the distribution extends up to 6σ, i.e. $b = 18\varepsilon$. The normalization of the distribution function to unity gives

(*a*)

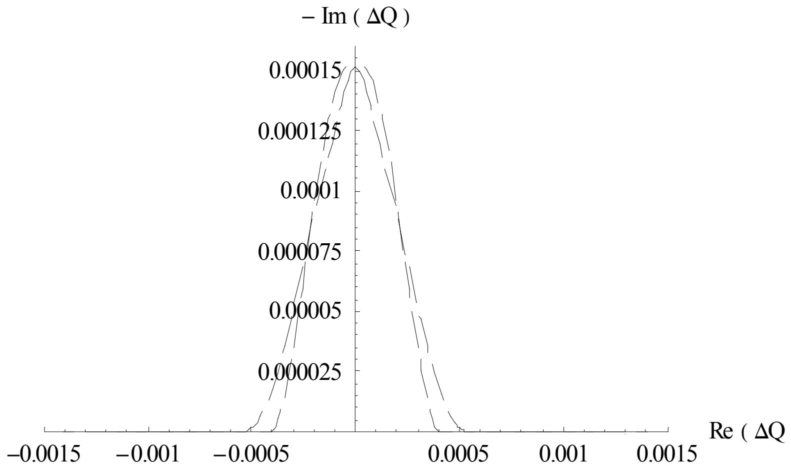
− Im (ΔQ)
0.00015
0.000125
0.0001
0.000075
0.00005
0.000025
Re (ΔQ)
−0.0015
−0.001
−0.0005
0.0005
0.001
0.0015

(b)

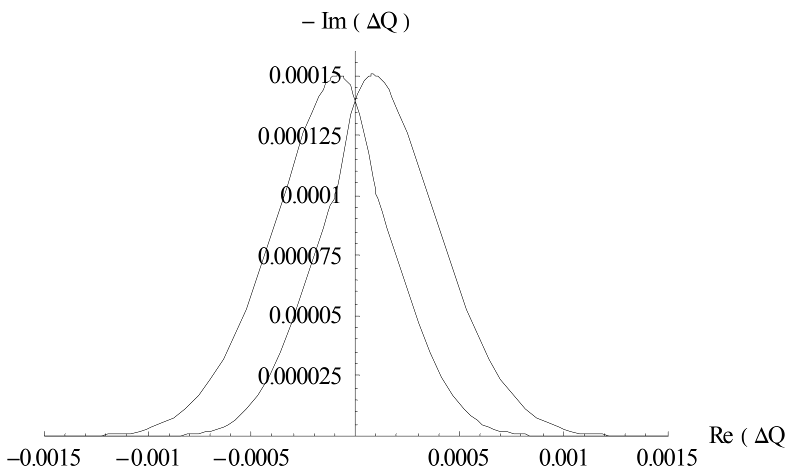
− Im (ΔQ)
0.00015
0.000125
0.0001
0.000075
0.00005
0.000025
Re (ΔQ)
−0.0015
−0.001
−0.0005
0.0005
0.001
0.0015

(*c*)

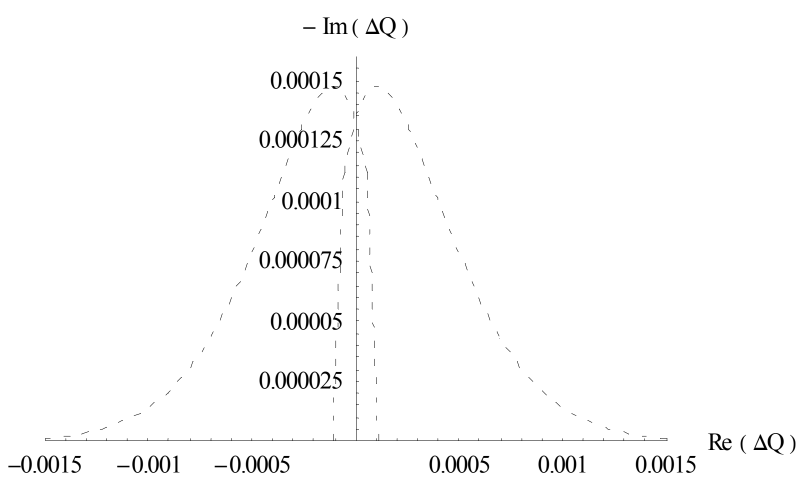
− Im (ΔQ)
0.00015
0.000125
0.0001
0.000075
0.00005
0.000025
Re (ΔQ)
−0.0015
−0.001
−0.0005
0.0005
0.001
0.0015

(*d*)

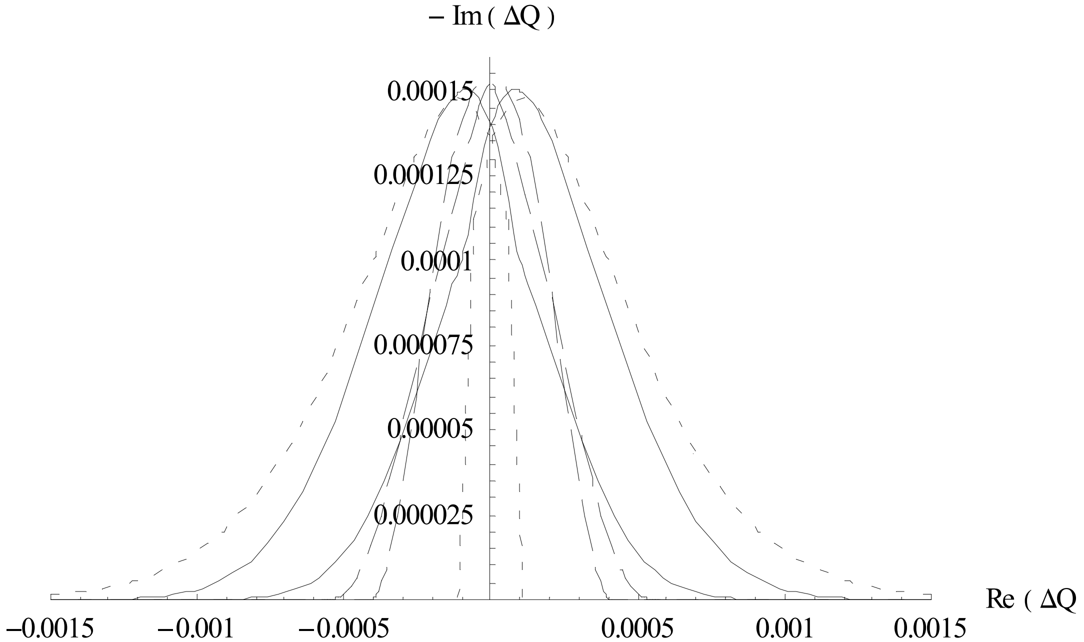

Figure 3: Stability diagrams (positive and negative detunings a_0) for the LHC at top energy (7 TeV) with maximum available octupole strength, for (*a*) the 2^{nd} order, (*b*) the 15^{th} order, (*c*) the Gaussian, and (*d*) all the distributions.

$$\int_{J_x=0}^{b} dJ_x \int_{J_y=0}^{b-J_x} dJ_y \, f\left(J_x, J_y\right) = \frac{a\,b^2}{(n+1)(n+2)} + \frac{d\,b^2}{(p+1)(p+2)} = 1 . \qquad (21)$$

The average of the action variable is equal to the emittance ($< J > = \varepsilon$), which gives

$$\int_{J_x=0}^{b} J_x \, dJ_x \int_{J_y=0}^{b-J_x} dJ_y \, f\left(J_x, J_y\right) = \frac{a\,b^3}{(n+1)(n+2)(n+3)} + \frac{d\,b^3}{(p+1)(p+2)(p+3)} = \varepsilon . \qquad (22)$$

It can be deduced from Eqs. (21) and (22) that

$$a = \frac{(n+1)(n+2)(n+3)(15-p)}{18\,b^2\,(n-p)}, \quad \text{and} \quad d = \frac{(p+1)(p+2)(p+3)(n-15)}{18\,b^2\,(n-p)} . \qquad (23)$$

As a and d must be positive to guarantee a positive density, it is seen from Eq. (23) that n must be larger than 15 and p must be smaller than 15. The case $n = 15$, $p = 0$ corresponds to that examined in the previous sections. Using Eq. (7), the horizontal beam profile is

$$g(x)=\frac{1}{9\pi(n-p)\sqrt{2b}}\left\{\begin{array}{l}\frac{(n+2)(n+3)(15-p)\left[2^{n+1}(n+1)!\right]^2}{(2n+3)!}\left(1-\frac{x^2}{2b}\right)^{n+\frac{3}{2}}\\+\frac{(p+2)(p+3)(n-15)\left[2^{p+1}(p+1)!\right]^2}{(2p+3)!}\left(1-\frac{x^2}{2b}\right)^{p+\frac{3}{2}}\end{array}\right\}. \qquad (24)$$

Let's take as an example the case where n = 16 and p = 2, i.e. the smallest integers which can be considered. The case p = 2 corresponds to the most populated tails. The distribution which is quasi-parabolic encompasses 2% of the particles. The transverse beam profiles for the case n = 16 and p = 2, and for the Gaussian distribution are plotted in Fig. 4. As can be seen in Fig. 4, this function is very close to a Gaussian distribution. The more populated tails are apparent on Fig. 5, where the growth below 6σ is much faster than the exponential in this range. Actually the new distribution passes below the Gaussian for a distance larger than 5.92σ. The new distribution provides a good example of a distribution more populated than the Gaussian in the tails. Choosing a value of p larger than 2, would provide a distribution closer to the Gaussian at larger amplitudes.

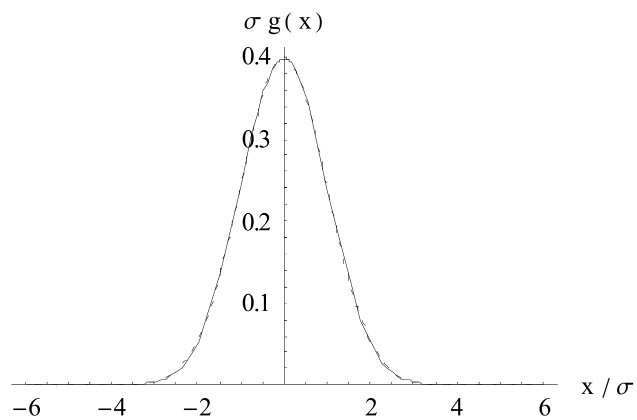

Figure 4: Transverse beam profile for the case n = 16 and p = 2 (full curve) and the Gaussian distribution (dotted curve).

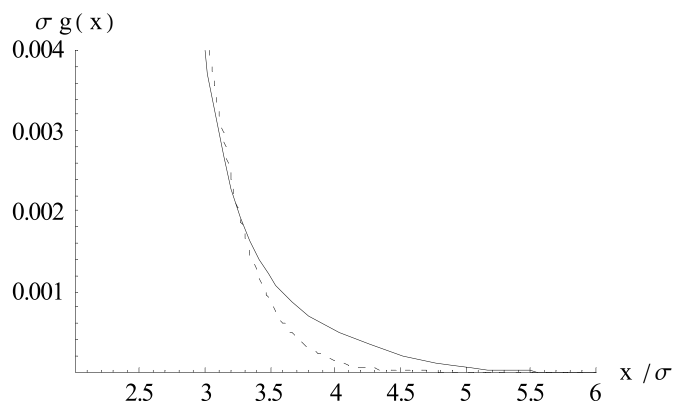

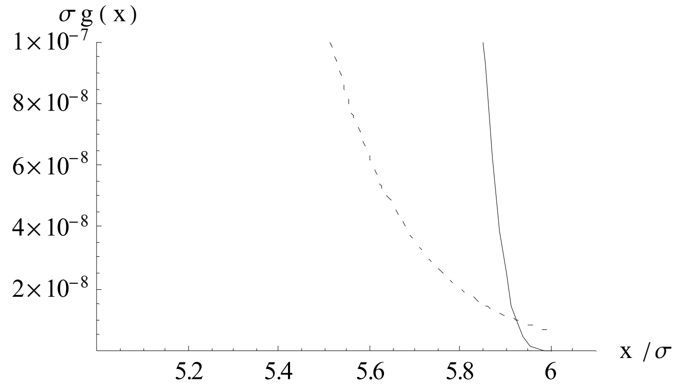

Figure 5: Zoom of the tails of the transverse beam profiles for the case n = 16 and p = 2 (full curve) and the Gaussian distribution (dotted curve).

For the case where a pth order distribution function is added to an nth order distribution, the dispersion equation of Eq. (1) can be re-written as

$$\Delta Q_{coh}^{x} = - \frac{a_0 / b}{n\,a\,I_n(c,q) + p\,d\,I_p(c,q)} \; . \tag{25}$$

In the case where n = 16 and p = 2, $I_p(c,q)$ is given by Eq. (14), while $I_n(c,q)$ is given by (using *Mathematica* [4]) Eq. (A2) of Appendix 2.

The stability diagram for the case n = 16 and p = 2 is plotted in Fig. 6 for the case of the LHC at top energy with maximum available octupole strength, and is compared to the Gaussian case in Fig. 7. It can be seen from Fig. 7 that the stability diagram has been considerably enlarged compared to the Gaussian case, even if the transverse beam profile extends only up to 6σ (compared to infinity for the Gaussian distribution) and that there is no visible difference between the two profiles on Fig. 4.

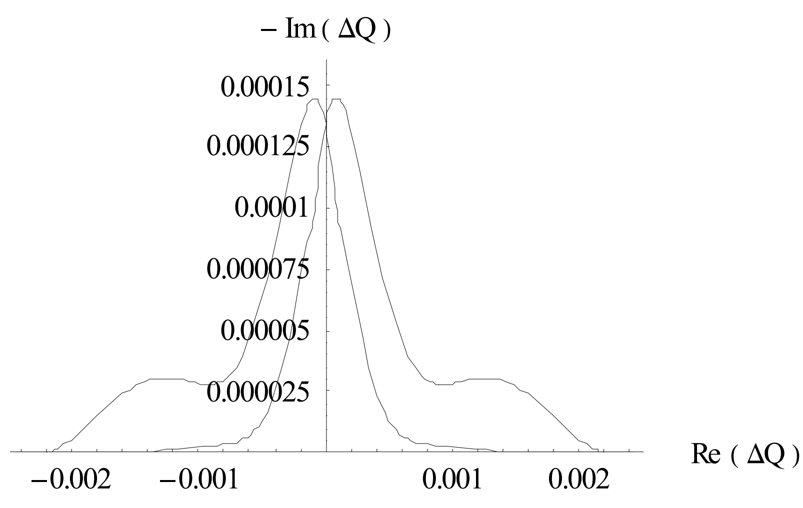

Figure 6: Stability diagrams (positive and negative detunings a_0) for the LHC at top energy (7 TeV) with maximum available octupole strength, for the case n = 16 and p = 2.

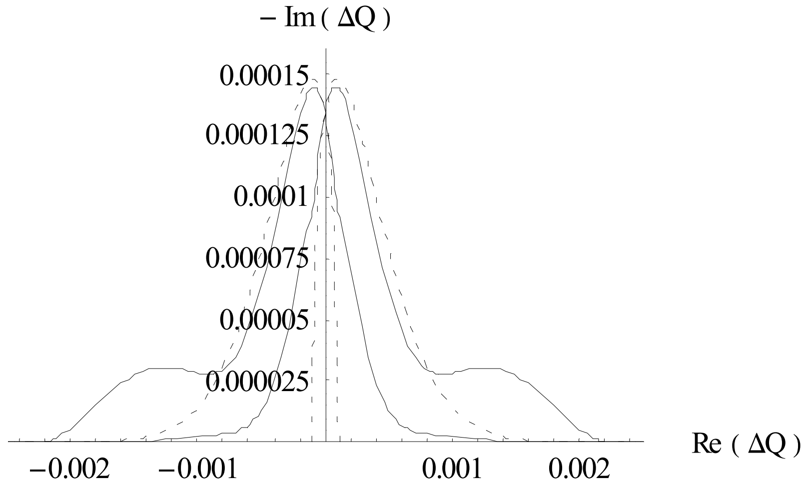

Figure 7: Stability diagrams (positive and negative detunings a_0) for the LHC at top energy (7 TeV) with maximum available octupole strength, for the case n = 16 and p = 2 (full curve) and the Gaussian distribution (dotted curve).

6 CONCLUSION

The stability diagram for Landau damping with two-dimensional betatron tune spread from octupoles has been computed for the 15th order distribution function, whose transverse beam profile extends up to 6σ, as it is foreseen to be the case in the LHC at top energy with the nominal collimator settings. The new result has been compared to the ones already obtained with the 2nd order and Gaussian distribution functions. As expected the stability diagram of the 15th order distribution lies between the 2nd order and the Gaussian distributions, but now beam stability is computed with the "self-consistent" beam distribution, i.e. set by the collimator settings (at 6σ). It is seen in Fig. 3(d) that a factor of 2 is gained for the real part of the coherent tune shift compared to the case with the 2nd order distribution function. As already mentioned in Ref. [3], the presence or not of the high-amplitude tails in the distribution can substantially affect the amount of Landau damping. These stability diagrams should therefore be used with great care for beam stability analyses/predictions in real machines. The case of a distribution extending up to 6σ (as the 15th order distribution) but with more populated tails than the Gaussian distribution has been considered and revealed a significant enhancement of the stable region compared to the Gaussian case (see Fig. 7). This may be the case in reality in proton machines due to diffusive mechanisms.

REFERENCES

[1] J. Scott Berg and F. Ruggiero, "Landau Damping with Two-Dimensional Betatron Tune Spread", CERN SL-AP-96-71 (AP), December 1996.

[2] E. Métral, "Coupled Landau Damping of Transverse Coherent Instabilities in Particle Accelerators", Ph.D. Thesis, Joseph Fourier University of Grenoble (France), 1999.

[3] J.S. Berg and F. Ruggiero, “Stability Diagrams for Landau Damping”, PAC’97, Vancouver, B.C., Canada, 12-16 May 1997.

[4] S. Wolfram, *Mathematica*, A System for Doing Mathematics by Computer, Second Edition, Addison Wesley (1991).

APPENDIX 1: Dispersion integral for the 15th order distribution function solved using *Mathematica* [4]

$$
\begin{aligned}
I_{15}(c,\ q) = & -\frac{1}{86486400\,(-1+c)^2\,c^{15}}\,(c\,(360360\,(-1+c)\,c^{14} + 5405400\,(-1+c)\,c^{14}\,q + 60\,(-1+c)\,c^{13} \\
& (-1355479 + 1986109\,c)\,q^2 + 280\,c^{12}\,(1115239 + c^2\,(-3931302 + 2816063\,c))\,q^3 \\
& + 910\,c^{11}\,(935059 + c^3\,(-4280776 + 3345717\,c))\,q^4 + 10920\,c^{10}\,(158183 + c^4\,(-890014 + 731831\,c))\,q^5 \\
& + 20020\,c^9\,(134159 + c^5\,(-895044 + 760885\,c))\,q^6 + 28600\,c^8\,(113567 + c^6\,(-876050 + 762483\,c))\,q^7 \\
& + 32175\,c^7\,(95549 + c^7\,(-836464 + 740915\,c))\,q^8 + 257400\,c^6\,(8837 + c^8\,(-86540 + 77703\,c))\,q^9 \\
& + 108108\,c^5\,(12059 + c^9\,(-130600 + 118541\,c))\,q^{10} + 216216\,c^4\,(2627 + c^{10}\,(-31172 + 28545\,c))\,q^{11} \\
& + 30030\,c^3\,(6061 + c^{11}\,(-78192 + 72131\,c))\,q^{12} + 120120\,c^2\,(337 + c^{12}\,(-4696 + 4359\,c))\,q^{13} \\
& + 180180\,c\,(31 + c^{13}\,(-464 + 433\,c))\,q^{14} + 360360\,(1 + c^{14}\,(-16 + 15\,c))\,q^{15}) + \\
& 360360 \\
& ((c+q)^{16}\,\mathrm{Log}[1+q] - (c+q)^{16}\,\mathrm{Log}[c+q] - \\
& q^2\,(120\,c^{14} + 560\,c^{13}\,q + 1820\,c^{12}\,q^2 + 4368\,c^{11}\,q^3 + 8008\,c^{10}\,q^4 + 11440\,c^9\,q^5 + 12870\,c^8\,q^6 \\
& + 11440\,c^7\,q^7 + 8008\,c^6\,q^8 + 4368\,c^5\,q^9 + 1820\,c^4\,q^{10} + 560\,c^3\,q^{11} + 120\,c^2\,q^{12} + 16\,c\,q^{13} \\
& + q^{14} - 16\,c^{15}\,(3 + q\,(3+q))\,(1 + q\,(1+q)\,(2+q)\,(1 + q\,(1+q)^2)\,(2 + q\,(2+q)))\,(5 \\
& + q\,(10 + q\,(10 + q\,(5+q)))) \\
& + c^{16}\,(120 + \\
& q \\
& (1120 + \\
& q\,(5460 + q\,(17472 + q\,(40040 + q\,(68640 + q\,(90090 + q\,(91520 + q\,(72072 + q\,(43680 \\
& + q\,(20020 + q\,(6720 + q\,(1560 \\
& + q\,(224 + 15\,q)))))))))))))))) \\
& (-\mathrm{Log}[q] + \mathrm{Log}[1+q]))).
\end{aligned}
\tag{A1}
$$

APPENDIX 2: Dispersion integral for the 16th order distribution function solved using *Mathematica* [4]

$$
\begin{aligned}
I_{16}(c,\ q) = &-\frac{1}{98017920(-1+c)^2 c^{16}} \big(c\big(95055452\,c^{14} q^2 + 393595660\,c^{13} q^3 + 1163170610\,c^{12} q^4 + 2578262050\,c^{11} q^5 \\
&+ 4413221540\,c^{10} q^6 + 5933879380\,c^9 q^7 + 6322305275\,c^8 q^8 + 5348932875\,c^7 q^9 + 3578318172\,c^6 q^{10} \\
&+ 1871673804\,c^5 q^{11} + 750011262\,c^4 q^{12} + 222492270\,c^3 q^{13} + 46066020\,c^2 q^{14} + 5945940\,c q^{15} \\
&+ 360360\,q^{16} - \\
&c^{15} \\
&\big(360360 + \\
&q \\
&\big(5765760 + \\
&17\,q\big(13726712 + \\
&q\big(81328740 + q\big(312266920 + 13\,q\big(65454130 + q\big(132873720 + 11\,q\big(18782260 + q\big(22713400 + \\
&3\,q\big(7166175 + 2\,q\big(2651100 \\
&+ 7\,q\big(217062 + q\big(94572 + \\
&5\,q\big(6061 + 2\,q\big(674 \\
&+ 93\,q + 6\,q^2\big)\big)\big)\big)\big)\big)\big)\big)\big)\big)\big)\big)\big)\big)\big) + \\
&c^{16} \\
&(360360 + \\
&q \\
&(5765760 + \\
&q(138298652 + q(988992920 + q(4145367030 + 13\,q(914392360 + q(1919374660 \\
&+ 11\,q(277802760 + q(341915875 + 6\,q(54678300 \\
&+ q(40898166 + 7\,q(3378420 + q(1482847 \\
&+ 10\,q(47814 + q(10691 \\
&+ 6\,q(247 \\
&+ 16\,q)))))))))))))))))\big) + \\
&360360 \\
&\big((c+q)^{17}\,\mathrm{Log}[1+q] - (c+q)^{17}\,\mathrm{Log}[c+q] - \\
&q^2\big(136\,c^{15} + 680\,c^{14} q + 2380\,c^{13} q^2 + 6188\,c^{12} q^3 + 12376\,c^{11} q^4 + 19448\,c^{10} q^5 \\
&+ 24310\,c^9 q^6 + 24310\,c^8 q^7 + 19448\,c^7 q^8 + 12376\,c^6 q^9 + 6188\,c^5 q^{10} + 2380\,c^4 q^{11} \\
&+ 680\,c^3 q^{12} + 136\,c^2 q^{13} + 17\,c q^{14} + q^{15} - 17\,c^{16}(2+q)(2+q(2+q))(2 \\
&+ q(2+q)(2+q(2+q)))(2+q(2+q)(2+q(2+q))(2+q(2+q)(2+q(2+q)))) + \\
&c^{17} \\
&(136 + \\
&q(1360 + \\
&q(7140 + q(24752 + q(61880 + q(116688 + q(170170 + q(194480 + q(175032 \\
&+ q(123760 + q(68068 + q(28560 \\
&+ q(8840 + q(1904 \\
&+ q(255 + 16\,q)))))))))))))))\big) \\
&(-\mathrm{Log}[q] + \mathrm{Log}[1+q])\big)\big).
\end{aligned}
\tag{A2}
$$